methane

MDPI

Article

A Study on the Heterogeneity and Anisotropy of the Porous Grout Body Created in the Stabilization of a Methane Hydrate Reservoir through Grouting

Yuchen Liu * and Masanori Kurihara

Faculty of Science and Engineering, Waseda University, Tokyo 1698555, Japan; kurihara.m@waseda.jp
* Correspondence: liu_yuchen@aoni.waseda.jp

Abstract: To solve the sand problem during the depressurization of methane hydrate (MH), we proposed a method to build a porous grout body with sufficient permeability and strength around the wellbore through inhibitor pre-injection and grouting, and verified its effectiveness and potential in our previous research using artificial cores created with silica sand and alternative hydrates such as TBAB- hydrate and *iso*-butane hydrate. However, all of the artificial cores mentioned above were created with high homogeneity, injected, cured, and had their physical properties measured in the vertical direction, which differs from real reservoir conditions. To investigate the effects of grouting in a more realistic fluid flow, we conducted further experiments using horizontal 1D cores, 1D cubic models, and a 2D cross-sectional model mimicking the near wellbore. These experiments revealed that (1) the generated gas somewhat suppressed the effects of grouting as in the case of previous experiments, and (2) grouted reservoirs would be heterogenous and anisotropic due to the fluid densities and the distribution of grout particles and turbidite sediments, but sufficient permeability and satisfactory strength could still be attained. The above series of experiments demonstrated that our method has the potential to effectively produce actual MH, preventing sand problems even in heterogeneous and anisotropic grouted reservoirs.

Keywords: methane hydrate; sand problem; grout material; formation stabilization; porous grout body; *iso*-butane hydrate; grouting experiment; physical properties; heterogeneity; anisotropy

Citation: Liu, Y.; Kurihara, M. A Study on the Heterogeneity and Anisotropy of the Porous Grout Body Created in the Stabilization of a Methane Hydrate Reservoir through Grouting. *Methane* **2024**, *3*, 331–345. https://doi.org/10.3390/methane3020018

Academic Editor: Patrick Da Costa

Received: 28 February 2024
Revised: 23 April 2024
Accepted: 30 April 2024
Published: 21 May 2024

1. Introduction

Methane hydrate (MH) is expected to be one of the new natural gas resources in the future due to its enormous amount of available resource and small uneven distribution [1]. Depending on the formation types, MHs are classified into (1) the sand layer-type, which fills in the pores of subsea formations or is distributed under the permafrost, and (2) seabed-type, which is distributed on the sea floor or in the extremely shallow seabed sediment [2]. During the past few decades, field production tests of sand layer MH have been conducted in several countries, suggesting the promise of MH dissociation and production by using the depressurization method [3]. However, MH reservoirs are usually located in very shallow formations without sufficient natural consolidation, and MH in porous media plays a role in bonding sand grains. Therefore, the consolidation of sand grains is weakened or lost, associated with the dissociation of MH through depressurization, resulting in the easy separation and migration of sand grains. This causes much more serious sand problems than those in conventional oil and gas production [4]. For sand control in MH productions, gravel pack screens and GeoFORM^{TM} (Baker Hughes Inc., Houston, TX, USA) have been installed in recent offshore production tests, but their effect is extremely insufficient [5].

To solve this problem, we proposed a new method to stabilize MH reservoirs by injecting (a) grout material(s) into the pores to artificially bond sand grains, creating (a) porous grout body(ies) around the wellbore (Figures 1 and 2) which can stop and prevent sand migration from further reservoir volume into the wellbore. Grouting is a method

commonly used in civil engineering but has never been attempted for MH production. The key points of our method are that (1) grout material can be injected into a reservoir with high MH saturation, (2) injected grout material can consolidate sand grains even in the high MH saturation conditions, (3) grouted MH reservoirs can have sufficient permeability for fluid production, and (4) grouted MH reservoirs can have sufficient strength even after MH dissociation.

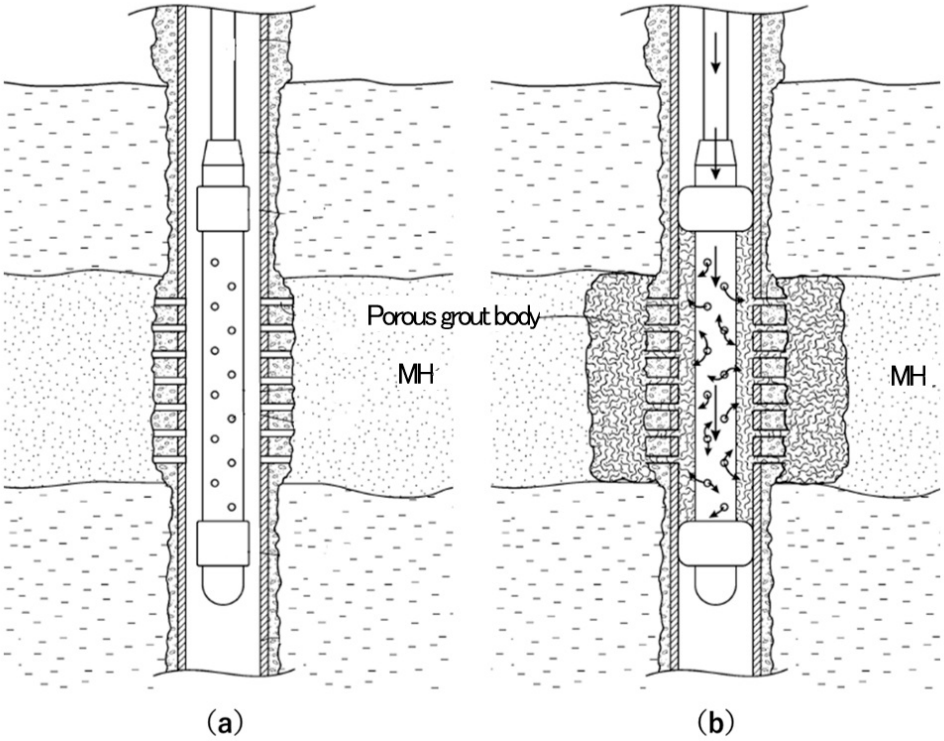

Figure 1. Image of grout injection for MH reservoir stabilization. (**a**) Before grouting. (**b**) After grouting. Reprinted/adapted with permission from Ref. [6]. 2018, Liu and Kurihara.

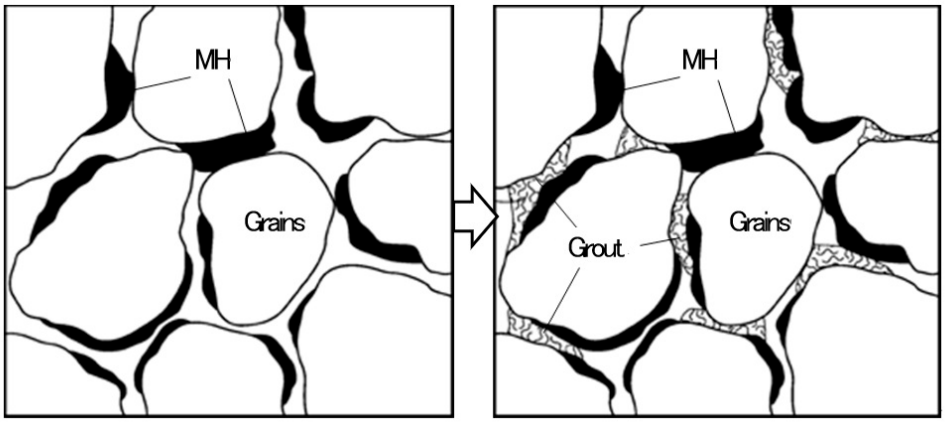

Figure 2. Image of solid phase distribution before and after grouting in MH reservoir. Reprinted/adapted with permission from Ref. [6]. 2018, Liu and Kurihara.

To verify the effectiveness of this method, we attempted to conduct core experiments using alternative hydrates that can be generated at lower pressures than MH. Several alternative hydrates have been used for MH experiments, such as the hydrates of tetrahydrofuran (THF), 1,1-Dichloro-1-fluoroethane (R-141b), Tetra-n-butylammonium bromide (TBAB), and propane (C_3H_8) [7–10]. In our previous experiments, we applied this grouting method to the artificial cores filled with TBAB hydrate (TH), which could be easily

generated in high saturation (up to 100%) with low erosivity to PVC and cast acrylic parts. It was confirmed that the four key points mentioned above could be accomplished under conditions of low or atmospheric pressure in conjunction with pretreatment by an inhibitor injection [11]. Additionally, we used *iso*-butane hydrate (*i*-BH) which has a lower equilibrium pressure than propane hydrate, instead of MH and TH, to examine the effects of the generated gas during and after the chemical injection. We clarified that the gas phase generated at the interface between *i*-BH and chemicals, such as inhibitor and grout materials, somewhat prevented further injection and pushed back the injected grout materials out of the cores during curing, but approximately two-thirds of the strengths of the TH cores with sufficient permeabilities were still achievable due to the operation conditions [12].

However, most of the above research was conducted as quantitative experiments using vertical cylindrical core cells, creating artificial cores through water pluviation from the top, injecting inhibitors and grout materials from the bottom, and recovering generated gas and permeated chemicals from the top, which were cured vertically and their physical properties were measured in the vertical (*Z*-axis) direction. It was significantly different from real reservoir conditions, which are usually considered to have horizontal or radial fluid flow. In the case of horizontal flow, grouted reservoirs were assumed to be much more heterogeneous than vertical cores, since chemicals would concentrate in limited portions due to the different densities between formation water, injected chemicals, and gas generated from MH dissociation. Additionally, the particles of grout materials in low-speed flow would sediment onto the upper surface of sand grains before their hydration (consolidation) [13]. This was assumed to lead to anisotropy in the grouted/cured reservoir.

In this research, we conducted experiments using horizontal 1D cores, 1D cubic models, and a 2D cross-sectional model. Chemicals were injected horizontally, which is more realistic to real wellbore fluid flow. Cores and models were cured and their physical properties were measured in the X, Y, and Z directions. We clarified qualitatively that the heterogeneities and anisotropies in a grouted MH reservoir depends on the reservoir/operation conditions.

2. Methods

Since the experiments aimed to develop and refine our grouting method, similar conditions (materials, temperature/pressure, etc.) to the previous experiments were used so that the results could be compared with our old data.

2.1. Materials

2.1.1. Artificial Cores/Models

Artificial cores/models were created through water pluviation, dropping No. 7 Tohoku silica sand ($d50$ = 128 μm) into formation waters. No. 7 Tohoku silica sand was also used in our previous experiments since its grain size distribution is close to that of the MH reservoir in Nankai trough, Japan [14] (Figure 3). In addition, two types of formation water were used: (1) pure water (salinity 0%) and (2) a 5% NaCl solution, depending on the experiment conditions. Pure water was used to generate gas hydrate (Section 2.1.2), while the 5% NaCl solution was used for non-hydrated cores/models due to its effectiveness in preventing freezing. Initially, the initial salinity of the formation water had confirmed no damage or expansion to the effectiveness of grouting, since it would be replaced by the chemical injection [11].

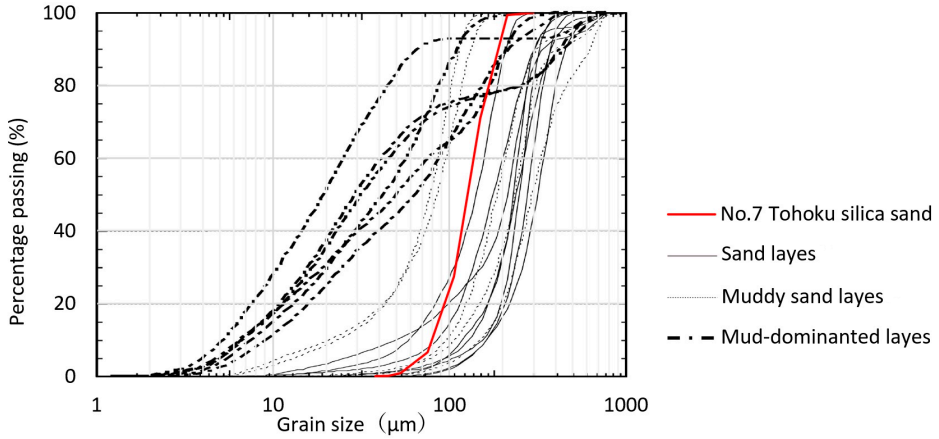

Figure 3. Grain size distributions of Nankai trough sediments and silica sand. Reprinted/adapted with permission from Refs. [11,15]. 2010, 2020, The Japanese Association for Petroleum Technology.

2.1.2. Alternative Hydrate

Alternative hydrates are expected to be easily generated in the pores to reproduce the conditions of MH reservoirs, such as saturation, initial effective permeability, temperature, and pressure. However, pressures of MH reservoirs are usually up to 10 MPa, making it difficult and cumbersome to create apparatus in university labs according to the Japanese high-pressure gas regulations. Therefore, *iso*-butane hydrate (*i*-BH) was used as the alternative hydrate as in previous experiments, which can be generated at a reasonably low pressure and reproduce the behaviors of gas generation during the chemical injection and curing.

Iso-butane has the lowest equilibrium pressure among the (C1-C4) single-component gas hydrates. The equilibriums of the gas, liquid, and hydrate at different salinities are shown in Figure 4. In pure water, *i*-BH could be generated at conditions lower than 2 °C/168 kPa, while its stability zone shifts to lower temperatures in higher salinity, suggesting that NaCl could act as an inhibitor for its hydration. Additionally, the *iso*-butane used in this research was a 95% fuel gas for outdoor winter sports, which was much cheaper but had been successfully applied for *i*-BH generation/injection experiments without any influence from impurities [12].

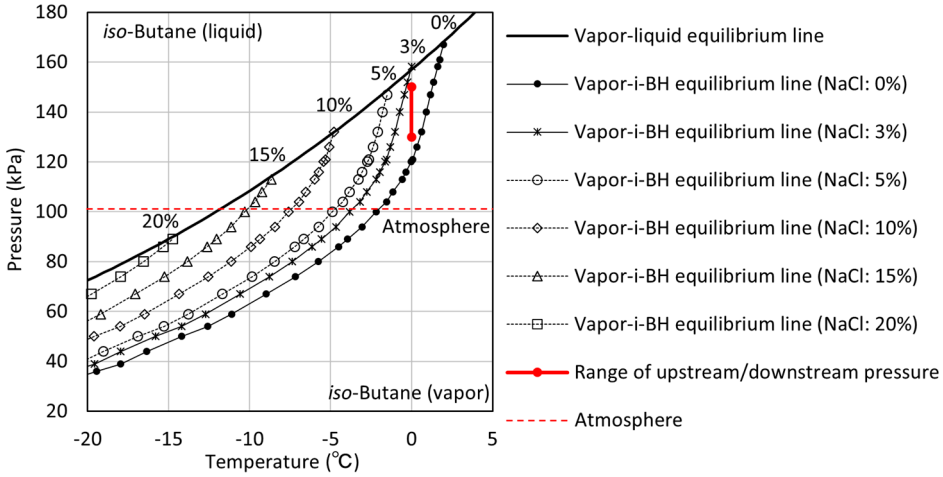

Figure 4. Equilibriums of *iso*-butane and *i*-BH with different inhibitor (NaCl) concentrations [12,16–18]. Reprinted/adapted with permission from Ref. [12]. 2023, The Japanese Association for Petroleum Technology.

2.1.3. Injected Chemicals

Chemical injections in the experiments were conducted in 2 steps: (1) pretreatments to improve the permeabilities of MH reservoirs through inhibitor pre-injection, and (2) grout

injections for sand grain consolidation, planned based on our previous results and discussions [11]. In step 1, NaCl solutions were used as the inhibitor because of their effect on moving the gas hydrate (MH/*i*-BH) equilibriums, and the concentrations were determined to be 20% for a higher effect. On the other hand, a cement-type grout material ($d50$ = 1.5 μm) with a dispersant recommended by the cement manufacturer was used in step 2, and an accelerator (GA-01) was used for low-temperature curing. All of the conditions of chemical preparation (components, concentrations, temperatures, procedures, etc.) were similar to our previous experiments, allowing for comparison of the data and results with the previous study (Table 1).

Table 1. Parameters of chemical preparation. Reprinted/adapted with permission from Ref. [11]. 2020, The Japanese Association for Petroleum Technology.

Chemicals	Substance/Conditions
Inhibitor	NaCl solutions @ 20%
Grout material	Main: cement-based grout material ($d50$ = 1.5 μm) Additive: manufacturer recommended dispersant Accelerator: GA-01 provided by Japan E&P international corporation
Temperature	Mixed/stirred @ 25 °C; injected @ 0 °C
Stirring	7000 rpm @ 1 atm for 5 min

2.2. Apparatus and Models

In real MH reservoirs, wellbore fluid flows, including injection and production, can be considered the integration of horizontal flows, where horizontal permeabilities are much more important than vertical ones. Additionally, formations around the wellbore are subjected to vertical compressive stress, including the effective stress significantly increased by depressurization. Therefore, in these experiments, apparatus for 1D cores, 1D cubic models, and a 2D cross-sectional model were created for *i*-BH generation, chemical injection, curing, and physical property measurement in various directions. Furthermore, the auxiliary units/kits, such as the water discharger, common-rail gas feeder, permeability measurer kit, pressurization unit, cooling system, and chemical injection and fluid recovery unit, were the same as in our previous experiments [11,12].

2.2.1. One-Dimensional Cores

One-dimensional cores were created by using the water pluviation method in our old core cells, which had a diameter of 30 mm and a height of 70 mm. These cores were compact enough to be created homogeneously. To avoid the heterogeneities caused by settling velocities of different grains sizes, sand drops were kept at extremely low rates, and the water surfaces were timely adjusted to be approximately 1 cm higher than the top of the sand. Core cells after pluviation were capped with filters, perforated plates, O-rings, and heads so that chemicals could be injected/recovered through the cores without any sand migration. Since the core cells were independent and compact enough, they could be oriented in any direction for the experiments, such as horizontal injection/curing (Figure 5). Some of the cells were also equipped with sensors for temperature monitoring.

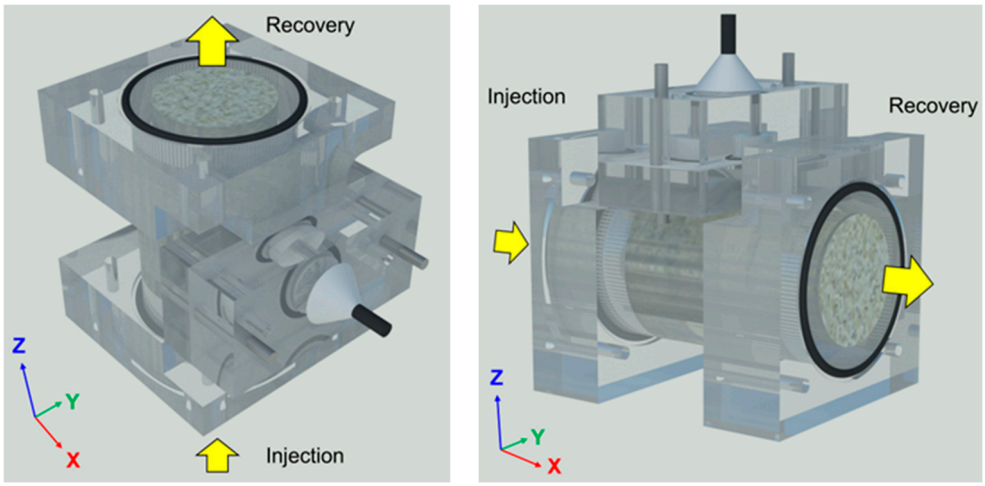

(**a**) (**b**)

Figure 5. 1D core cell blocks with different injection/curing directions: (**a**) vertical; (**b**) horizontal. Core cells could be changed to any direction or angle during/after injection.

2.2.2. One-Dimensional Cubic Models

One-dimensional cubic models were an expansion of the one-dimensional cores, with dimensions of 70 mm in length, 50 mm in width, and 70 mm in height. They were also compact enough to be created homogeneously and injected horizontally, but could be measured in three dimensions. Parts were assembled easily and reliably by using a liquid gasket, which was inspired by the assembly of vehicle engines. Sand was dropped from the top of the model, and a piece of 70 mm × 50 mm rubber sealing strip was used to prevent fluid leakage through the top of the sand. Since cubic molds do not have the same rigidity as cylinders (1D core cells), steel outside frames were installed to prevent expansion and deformation (Figure 6). Additionally, the physical properties could be measured by cutting the models into 50 mm cubic samples, or drilling cores in the X, Y, and Z directions.

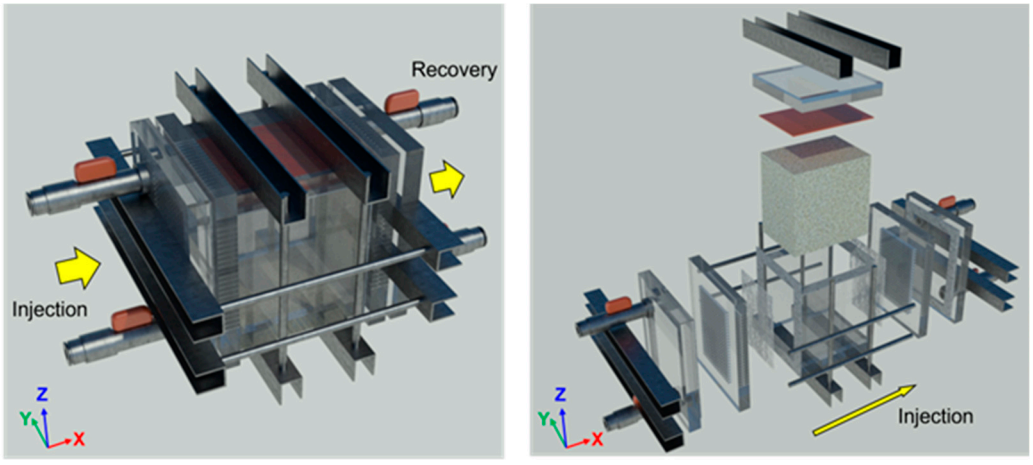

(**a**) (**b**)

Figure 6. 1D cubic models: (**a**) assembled and (**b**) disassembled.

2.2.3. Two-Dimensional Cross-Sectional Model

A 2D cross-sectional model was created for clarifying the heterogeneities of the porous grout body, described by the distributions of physical properties in each block. The basic configuration and mechanism were similar to our first 2D cross-sectional model created in 2018 [11] but with a greater thickness so that the physical properties in the Y direction could be easily measured. A rubber sealing strip was installed between the top of the sand layer

and the bottom of the cap to prevent fluid leakage, similar to the 1D cubic models. Steel frames were installed on both sides of the model to withstand the pressure of *iso*-butane, with lifting rings so that the model could be moved by a mini crane. Unlike the 1D cores or models, the 2D cross-sectional model could be cut into several blocks to clarify the distributions of the physical properties (Figure 7).

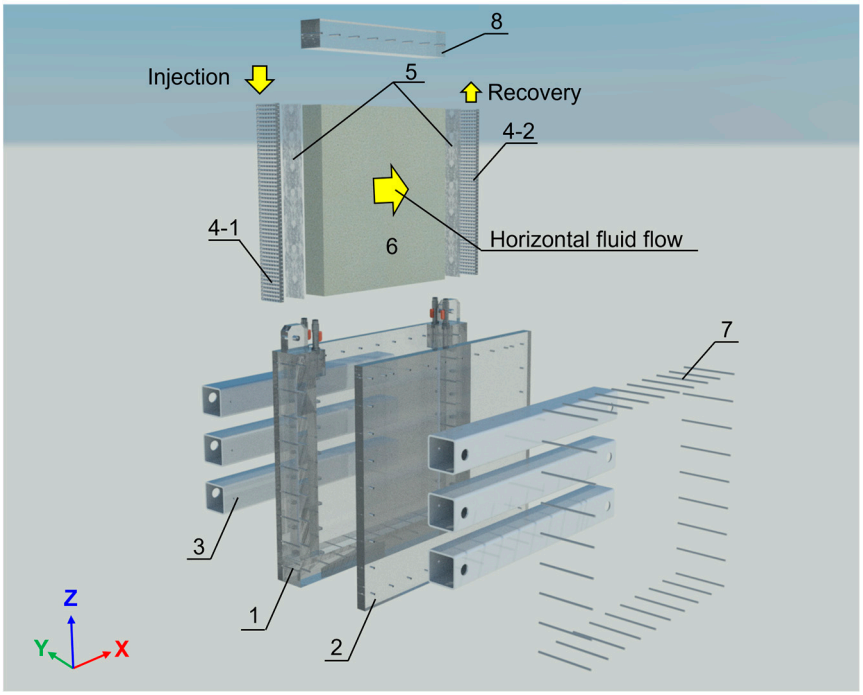

Figure 7. Image of 2D cross-sectional model: (1) back panel, (2) front panel, (3) steel frames, (4-1) perforated plate on wellbore side (casing), (4-2) perforated plate on forward reservoir side, (5) filters, (6) 2D reservoir model with silica sand and *i*-BH, (7) bolts, and (8) cap with 350 mm × 50 mm rubber sealing strip.

2.3. Operations and Measurement

2.3.1. Water Pluviation and *i*-BH Generation

All cores/models in the experiments were created by means of water pluviation using No. 7 Tohoku silica sand, as described in Section 2.2.1. Porosities were controlled to be 38.0% by adjusting the mass of sand and tapping on the cells until the sand tops were at the same height as the edge of the core cells or model molds. *i*-BH was generated in the pores using the "quantitative water discharging and ice replacement method", which was used in our previous research. The *i*-BH saturation was adjusted by controlling the initial water/ice saturation, which was highly correlated with the wet air flow for water discharging [12]. As the control parameter of water discharge, velocity (cm/s) at the flow direction was used instead of rate (mL/s), as it can be easily applied to cores/models of different sizes and shapes. The correlation between wet air flow (velocity) and the expected *i*-BH saturation is shown in Figure 8 and Equation (1). Since the actual *i*-BH saturation could not reach the theoretical value, especially when a large amount of water/ice remained, the *i*-BH saturation in this study was determined to be 40%. After the water was discharged, cores/models were moved to a −5 °C cooling water bath to freeze the pore water. *Iso*-butane gas was supplied for more than 4 days to generate *i*-BH, which was also determined according to our previous research.

$$S_{iBH} = -0.106(\ln v) + 0.3959 \ (S_{iBH} \leq 40\%) \quad (1)$$

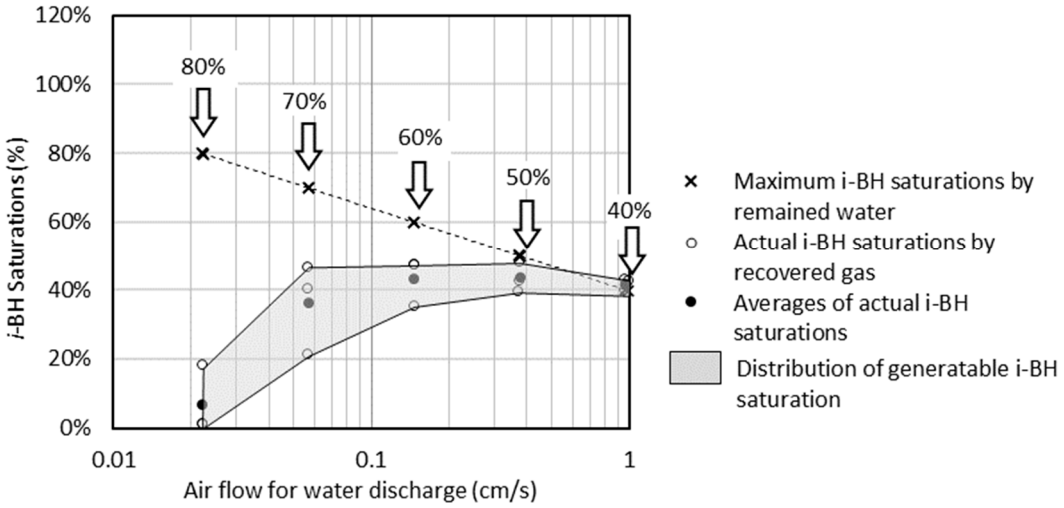

Figure 8. Correlations between wet air flow and expected *i*-BH saturation [12]. Reprinted/adapted with permission from Ref. [12]. 2023, The Japanese Association for Petroleum Technology.

2.3.2. Inhibitor and Grout Injections

Cores and models after gas generation were warmed to 0 °C to prepare for chemical injections. During injections, the temperature and pressure were kept within the stability zone using the cooling system and pressurization unit, while a differential pressure ΔP = 20 kPa was created between both sides of the cores/models (Figure 4). First, the inhibitor was injected as a pretreatment until the permeabilities were significantly improved according to the injection rate. Then, the grout materials were injected for approximately 2.5 or 5 pore volumes (PVs) depending on the core/model scales, monitored by the fluid (liquid) recovery volumes. Also, the gas recovery rates and volumes were monitored by the fluid recovery unit to decide the timing of chemical switching or injection stoppage. The cores/models after injection were cured at 0 °C while maintaining their orientations, connected to the pressurization and fluid recovery unit, as gas continued to be generated during curing.

2.3.3. Physical Property Measurement

The cores/models after curing were measured for their physical properties. In the case of 1D cores, both ends were cut approximately 1 cm before measurement to ensure that the grout material adhered to the filter would not interfere with the measurement data. For 1D cubic models and 2D cross-sectional models, they were cut into 50 mm blocks or cylindrical cores (φ = 30 mm) in the X, Y, and Z directions for measurement. These cut cores and blocks were measured for their effective permeabilities in dry air after water discharging, since *i*-BH was confirmed to be completely dissociated due to the gas recoveries. Dry densities and unconfined compressive strengths (UCSs) were also measured to evaluate the stabilization effects. UCS was chosen over triaxial compressive strength because (1) the UCS test is much simpler and allows for more efficient collection of strength data, and (2) natural formations or the grout body near/around the wellbore surface do not typically have sufficient lateral confining pressure, which is close to an unconfined compressive condition.

Based on the above, a flow chart and the experimental conditions of this study are, respectively, shown in Figure 9 and Table 2.

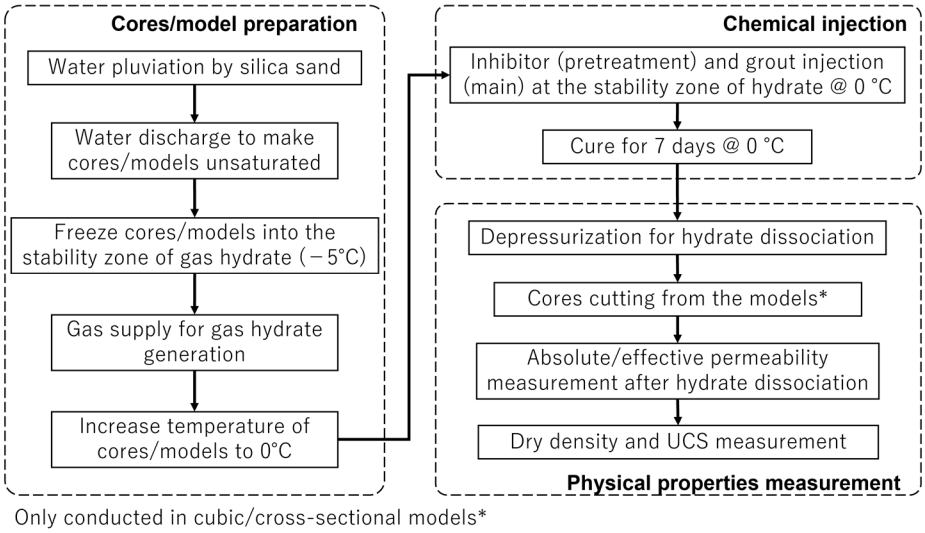

Figure 9. Flow chart of the experiment.

Table 2. Common experimental conditions.

Conditions	Substances/Details/Parameters
Materials for cores	No. 7 Tohoku silica sand (d50 = 128 μm), distilled water, and *iso*-butane hydrate (*i*-BH)
Porosity	38%
Initial *i*-BH saturation	0% or 40%
Salinity	5% for water-saturated cores as an antifreeze 0% for *i*-BH cores/models
Inhibitor	20% NaCl solution with red ink [1]
Grout material	Substances and concentrations shown in Table 1
Temperatures	−5 °C for *i*-BH generation; 0 °C for grouting/curing
Pressures	ΔP = 20 kPa within the *i*-BH stability zone
Injection stoppage	Inhibitor: significant increase in liquid recovery rates or gas generation stopped Grout material: 2.5 or 5 pore volumes (PVs)
Curing period	7 days [2]

[1] Ink was confirmed to have no effect on the experiments during our previous study. [2] An 8-day cured model was created due to operational reasons.

3. Results

3.1. Heterogeneities and Anisotropies in 1D Cores

In the experiments of 1D cores, seven cases (three cores in each case) were conducted, as shown in Table 3. Cases 1–3 were conventional vertical cores, injected from the bottom and recovered from the top. Among them, case 1 consisted of non-hydrate cores injected with grout material only, serving as a reference for the general performance of the material. Cases 2 and 3 consisted of 40% *i*-BH cores, which achieved approximately two-thirds of the strengths of case 1 (reference), as in our previous research. All of these cores had sufficient permeabilities for fluid production, but it was still unknown whether the vertical permeabilities could be used to simulate a radial wellbore fluid flow.

On the other hand, cases 4–6 involved horizontally injected cores under the same conditions (except fir direction), but all of them failed to be measured due to significant heterogeneities (Figure 10). In these cases, the grout material mainly passed through the lower parts of the cores, making them extremely hard, while the upper parts remained soft and required careful handling. The boundary of the well/poor-grouted portions was visible slightly above the position of the injection tube, suggesting that differences in densities between chemicals and formation water/gas caused significant heterogeneity in the distribution of chemicals and physical properties.

Table 3. Conditions and results of 1D core experiments. All data values of physical properties are averages of at least 3 cores in each case. Values in () show ratio to case 1.

Cases	Direction	*i*-BH Saturation (%)	Chemicals [1]	Effective Permeabilities [2] (mD)	Dry Densities (g/cm^3)	UCSs (MPa)	Heterogeneities or Anisotropies
1	Vertical [3]	0%	Grout only	789.15	1.94	3.70	None
2		40%	Grout only	826 (104.7%)	1.82 (93.8%)	2.33 (63.0%)	Low
3		40%	Inhibitor + grout	386 (48.9%)	1.88 (96.9%)	2.28 (61.6%)	Low
4	Horizontal	0%	Grout only	Failed to measure due to heterogeneity of cores			High
5		40%	Grout only				High
6		40%	Inhibitor + grout				High
7	Vertically injected [3] Horizontally cured	0%	Grout only	747.17 (94.7%)	1.93 (99.5%)	2.74 (74.1%)	Low

[1] Five pore volumes (PVs) were grouted. [2] After *i*-BH dissociation. [3] Injected from the bottom and recovered/monitored at the top.

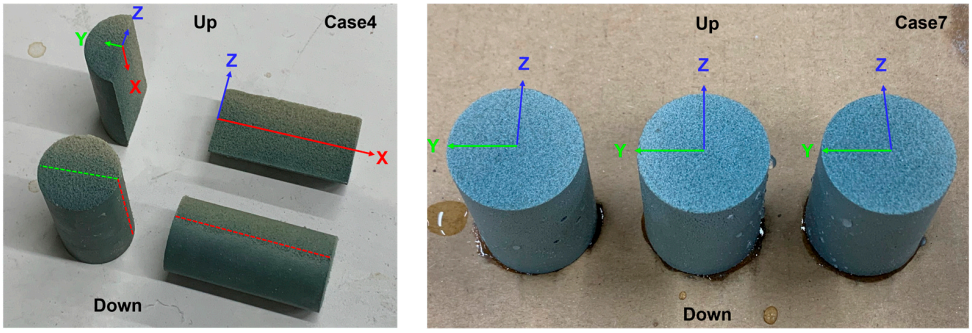

(**a**) (**b**)

Figure 10. Heterogeneity comparison of case 4 (**a**) and case 7 (**b**).

In addition, the cores in case 7 were injected vertically but cured horizontally to verify the effect of grout particle sedimentation. In this case, the cores were grouted homogeneously like the other vertically injected ones, but had lower permeabilities and UCSs than the vertically cured ones (case 1), even though they had similar densities. It was considered that the grout particles sedimented onto the upper surface of the sand grains before hydration, forming cement hydrate with different shapes, which would lead to anisotropy in the physical properties.

Since the table data on grout performances depending on the reservoir/operational conditions had been obtained from over 1000 vertical cores in our previous study, and horizontal permeabilities and vertical UCSs would be needed for a real MH reservoir, a quantitative conversion relationship needed to be found through further experiments.

3.2. Heterogeneities and Anisotropies in 1D Cubic Models

In the experiments of the 1D cubic models, three cases (7–9) were horizontally injected as the expansion of cases 4–6, with an improvement that the chemical tube was installed near the bottom, and an on–off valve was installed on the top of the side chamber, allowing the chemicals to completely fill the chamber and be injected homogenously. Compared to case 1, the horizontally injected models (case 8) had lower permeabilities than the vertical cores, while the permeabilities in the injected (X) direction were extremely higher than those of the cross (Y) or vertical (Z) directions (Table 4). It was considered that the grout particles were easily flocculated or sedimented into pores with lower fluid flow, particularly in the pores of the cross (Y) or vertical (Z) directions. Additionally, UCSs in the vertical (Z) direction were substantially higher than those in the horizontal (X and Y) directions for both non- and low-heterogenous models (case 8 and 10). This was attributed to the grout particles sedimenting onto the upper surfaces of the sand grains prior to their hydration, resulting in anisotropy in cement hydration, sand grain consolidation, and different physical properties of the grout body.

Table 4. Conditions and results of 1D cubic model experiments.

Cases	*i*-BH Saturation (%)	Chemicals [1]	Effective Permeabilities [2] (mD)	Dry Densities (g/cm^3)	UCSs (MPa)	Heterogeneities or Anisotropies
8 [3]	0%	Grout only	X: 622.1 (78.8%) Y: 465.4 (59.0%) Z: 422.8 (53.6%)	X: 1.91 (98.5%) Y: 1.91 (98.5%) Z: 1.91 (98.6%)	X: 3.10 (83.8%) Y: 3.07 (83.0%) Z: 4.43 (119.7%)	None
9	40%	Grout only	Failed to measure due to heterogeneity of models			High
10 [4]	40%	Inhibitor + grout	X: 275.0 (71.2%) Y: 423.6 (109.7%) Z: 338.0 (87.6%)	X: 1.90 (100.8%) Y: 1.89 (100.7%) Z: 1.90 (101.2%)	X: 2.64 (115.9%) Y: 2.88 (126.4%) Z: 3.18 (139.3%)	Low

[1] Pore volumes (PVs) of size 2.5 were grouted in the X direction. [2] After i-BH dissociation. [3] Values in the () show the ratio to case 1. [4] Values in the () show the ratio to case 3.

However, case 9 without inhibitor pretreatment still failed to be measured due to its significant heterogenies. Figure 11 shows the slice cuts of the case 9 model, where the grout material was found to have passed through a wormhole in the center of the model. Gas generation had been confirmed in our previous experiments and it tends to suppress the chemical injections especially in high-saturation portions, causing chemicals to be pushed out or concentrated into limited flow paths, such as wormholes. Therefore, reducing MH saturation through pretreatment is essential to achieve more homogenous grouting.

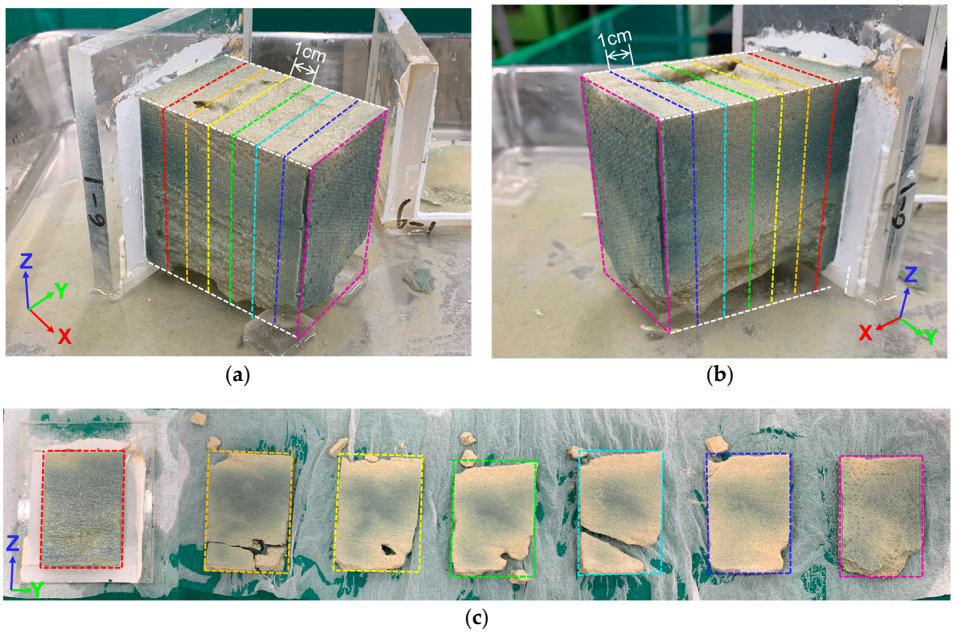

Figure 11. Heterogeneous injection in the case 9 model. A wormhole of the grout material was confirmed in the center of the model, and sand grains beside the wormhole were relatively poorly grouted. (**a**) right side, (**b**) left side, (**c**) slice cuts at 1 cm intervals. Color lines show the cut position of each slice.

3.3. Heterogeneities and Anisotropies in 2D Cross-Sectional Model

Since many MH reservoirs are confirmed to be formed in alternating layers of sand and clay, a 2D cross-sectional model experiment was conducted to clarify the heterogeneities and anisotropies in turbidite sediments. The model was created by using water pluviation, including multiple rapid sand drops with long time intervals, making the grain size distribution gradually/alternately changed in the vertical (Z) direction. Since the model aimed to clarify the effects of turbidite sediment, non-hydrate was generated in the pores to reduce other factors in the experiment. The model was completely horizontally grouted, cured for 8 days (including the last day at 25 °C) and divided into 42 blocks. Since all blocks could not be measured within a short time (to avoid changes in physical properties during the

measurement), three blocks each were sampled as representative of low/high anisotropies according to the striped sedimental patterns (Figure 12). The physical properties of each block are shown in Table 5, and the following results were obtained.

- Permeabilities in the injected (X) direction were confirmed to be significantly higher than those of the cross (Y) or vertical (Z) directions in all blocks, presenting a similar but more pronounced tendency compared to the 1D cubic models.
- Permeability ratios of (Y, Z)/X in the H segment were much lower than those of the L segment, which indicates that the turbidite sediments lead to more significant anisotropies in grouted models/reservoirs.
- Vertical (Z) UCSs were much higher than those of horizontal (X, Y) directions, aligning with trends observed in the 1D cubic models (case L1). Additionally, since the model was cured at 25 °C on the 8th day, UCSs in various samples exceeded the ranged measurable by the 10 kN universal tester, complicating discussions about the UCS ratios. Nevertheless, these data indicate extremely high strengths coupled with adequate permeabilities, and high performances in real MH reservoirs could be expected by applying wellbore heating during curing.
- Grouted turbidite sediments were confirmed to be much more heterogeneous and anisotropic compared to the homogenous models. Despite this, permeabilities in the injection/production (X) direction were sufficient for reservoir fluid flow, and the vertical (Z) UCSs which support the overburden formations were adequate to prevent sand problems during depressurization.
- Upper blocks near the wellbores (block A4–A6, G6) showed poor grouting, whereas lower blocks (block A1, A2, and G1–G3) were well grouted, with dense clusters of grout material (grout cake) observed at the bottom of the wellbore. This suggested that sedimentation of grout particles in the wellbores would lead to vertical heterogeneities, particularly near the wellbores which were the most stressed portion of the depressurized reservoir. To prevent the formation of grout cake, wellbore flushing by means of mud circulation should be conducted after the final grouting. However, the grout materials in the pores near the wellbore would be somewhat leached out during flushing, resulting in poor grouting and limited sand production.

Table 5. The physical properties of the blocks sampled from the 2D model. Values in the () show the ratio to the X direction.

Cases	Category	Effective Permeabilities [1] (mD)	Dry Densities (g/cm^3)	UCSs (MPa) [2]
L1	Low anisotropies	X: 445.3 Y: 324.2 (72.8%) Z: 197.6 (44.4%)	X: 1.81 Y: 1.79 (99.1%) Z: 1.77 (98.0%)	X: 3.74 Y: 3.73 (99.8%) Z: 5.69 (152.2%)
L2		X: 62.6 Y: 2.4 (3.8%) Z: 28.6 (45.7%)	X: 1.85 Y: 1.90 (103.0%) Z: 1.83 (98.7%)	X: >9.43 Y: 11.21 (-) Z: >9.39 (-)
L3		X: 186.9 Y: 102.5 (54.8%) Z: 143.6 (76.8%)	X: 1.78 Y: 1.84 (103.5%) Z: 1.77 (99.8%)	X: >8.58 Y: 6.96 (-) Z: 7.61 (-)
H1	High anisotropies	X: 39.2 Y: 2.1 (5.4%) Z: 0.3 (0.8%)	X: 1.89 Y: 1.93 (102.4%) Z: 1.86 (98.6%)	X: >9.28 Y: 10.94 (-) Z: >8.99 (-)
H2		X: 219.5 Y: 47.5 (21.6%) Z: 4.2 (1.9%)	X: 1.79 Y: 1.83 (102.5%) Z: 1.91 (106.6%)	X: >9.54 Y: 9.69 (-) Z: >9.38 (-)
H3		X: 155.8 Y: 22.8 (14.6%) Z: 0.6 (0.4%)	X: 1.84 Y: 1.89 (102.9%) Z: 1.89 (102.8%)	X: >9.19 Y: >11.66 (-) Z: >9.49 (-)

[1] After *i*-BH dissociation. [2] ">": data over the range measurable by the 10 kN universal tester.

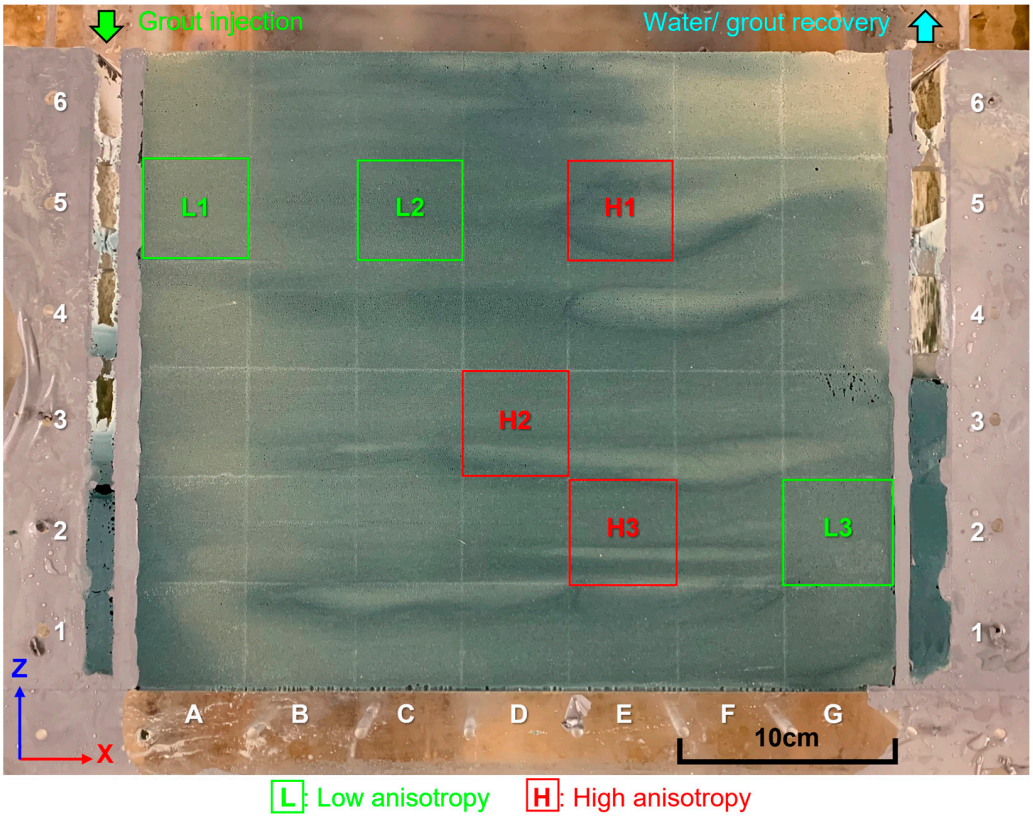

Figure 12. Sampled/measured blocks in heterogeneously grouted 2D cross-sectional model.

4. Discussion

In this research, 1D core, 1D cubic model, and 2D cross-sectional model experiments were conducted to elucidate the heterogeneities and anisotropies during/after grouting in a gas hydrate reservoir. Since gas generation during *i*-BH dissociation tends to suppress chemical injections and concentrate fluid flow into wormholes, cores and models with 40% *i*-BH saturation without pretreatment all failed to yield measurable physical properties due to significant heterogeneity. It was suggested that the grout body formed in a real MH reservoir without pretreatment would not assume a regular cylindrical shape, similar to channel injection, thus reducing the effectiveness of sand control. Additionally, since the gas generated tends to expel chemicals from the pores, *i*-BH cores with inhibitor pretreatments demonstrated approximately two-thirds of the UCSs of the non-hydrated cores, aligning with findings from the previous study.

However, in horizontally injected cores, the upper parts were significantly less well grouted than the lower parts, attributed to the higher density of the grout material compared to the formation water and gas. This implies that grouting might be challenging in the reservoir areas higher (shallower) than the upper packer of the injection tools or the upper half of the MH layer relative to the horizontal wells. Such insights could inform mechanical designs in terms of tools or wellbore planning, suggesting that horizontal wells should be drilled near the upper boundary of the MH layers to minimize ungrouted zones, which would lead to sand problems.

Moreover, permeabilities in the injection/production direction were confirmed to be extremely higher than in the normal or vertical directions in both 1D cubic models and the 2D cross-sectional model as a result of anisotropic flocculation and sedimentation of grout particles influenced by the injection fluid flow. Conversely, the vertical UCSs were markedly higher than those in the horizontal directions, attributable to the sedimentation of grout particles before their hydration. Since the horizontal (especially in the fluid flow direction) permeabilities and the vertical strength were much higher than those in other directions,

these would be advantageous for the propagation of depressurization and gas/water production, notwithstanding the increase in effective stress, to prevent sand problems.

Furthermore, the 2D cross-sectional model revealed that anisotropies in permeabilities of high-turbidity sediments were extremely greater than in other blocks, indicating that fines or clay layers horizontally distributed in reservoirs could impede vertical fluid flow, complicating chemical injections or gas production from upper/lower MH layers. Since many marine MH reservoirs are formed in turbidite sediments with MH layers ranging from 0.2 to 0.5 m [19,20], the grout body in each layer would not exceed this height. To enhance sand control and gas production from this type of reservoir, well completions using casing pipes with denser perforations or Johnson screens connected to all target MH layers are recommended.

Additionally, well flushing is considered essential to remove grout cake from the bottom or lower portion of the well, albeit at the expense of weakening the grout effect near the wellbore inner surface. This compromise should be accepted, given its critical role in facilitating subsequent depressurization operations and gas production, particularly in horizontal wells drilled near the top/upper portion of the MH layers with large bottom tareas.

5. Conclusions

This study successfully confirmed heterogeneities and anisotropies in physical properties during/after grouting in experiments involving 1D cores, 1D cubic models, and a 2D cross-sectional model. These variations were attributed to (1) differences in fluid densities (formation water/gas; chemicals), (2) chemical wormholes caused by gas generation, (3) the anisotropic distribution of grout particles in the pores governed by fluid injection and particle sedimentation, and (4) anisotropic grain size distribution in turbidite sediments. However, all of the cores and models with reduced saturations through pretreatment exhibited relatively homogeneous grouting, achieving satisfactory vertical strengths with sufficient horizontal permeabilities, which would be promising for solving sand problems during fluid production. Therefore, our grouting method demonstrates potential effectiveness in dissociating and producing actual MH, while preventing sand problems even in heterogeneous and anisotropic grout bodies. On the other hand, our experiments only assumed horizontal injection flow from a vertical wellbore, which limited the study of the heterogeneity and anisotropy caused by complex fluid flow, such as chemical injection from a horizontal wellbore drilled in a thin turbidite MH layer. For further research, we plan to conduct experimental studies assuming horizontal wells in a turbidite MH reservoir and perform numerical simulations of grout injections and gas production, taking into account the heterogeneous injection and the heterogeneities/anisotropies of the grout body, aiming for practical application and commercialization of this method.

Author Contributions: Conceptualization, methodology, experimental design, apparatus production, experimental operation, data curation, and writing—original draft preparation, Y.L.; writing—review and editing, M.K. All authors have read and agreed to the published version of the manuscript.

Funding: This research received no external funding.

Institutional Review Board Statement: Not applicable.

Informed Consent Statement: Not applicable.

Data Availability Statement: The data are only available on request due to restrictions outlined in the rules of the university and by the joint applicants, and research data protection regulations.

Acknowledgments: Some of the chemicals, apparatus, and tools used in the experiments were supplied by Japan E&P International Corporation.

Conflicts of Interest: The funders had no role in the design of the study; in the collection, analyses, or interpretation of data; in the writing of the manuscript; or in the decision to publish the results. The authors declare no conflicts of interest.

References

1. Satoh, M.; Maekawa, T.; Okuda, Y. Estimation of amount of methane and resources of natural gas hydrate in the world and around Japan. *J. Geol. Soc. Jpn.* **1996**, *102*, 959–971. [CrossRef]
2. Nagakubo, S. Methane Hydrate as a Domestic Energy Resource: Japan's Methane Hydrate R&D Program. *J. Geogr.* **2009**, *118*, 758–775.
3. Research Consortium for Methane Hydrate Resources in Japan; Nagao, J. Development of recovery enhancement method for methane hydrate production. In Proceedings of the Methane Hydrate Forum 2015, Tokyo, Japan, 1 October 2015. (In Japanese)
4. Yamamoto, K. Production Techniques for Methane Hydrate Resources and Field Test Programs. *J. Geogr.* **2009**, *118*, 913–934. [CrossRef]
5. Research Consortium for Methane Hydrate Resources in Japan; Yamamoto, K. About the 2nd offshore production test. In Proceedings of the Methane Hydrate Forum 2017, Tokyo, Japan, 29 November 2017. (In Japanese).
6. Liu, Y.; Kurihara, M. Production Method for Methane Hydrate Using Reservoir Grouting. JP Patent 7170725, 4 November 2022. U.S. Patent 11,492,884 B2, 8 November 2022.
7. Yun, T.S.; Santamarina, J.C.; Ruppel, C. Mechanical properties of sand, silt, and clay containing tetrahydrofuran hydrate. *J. Geophys. Res.* **2007**, *112*, 1–13. [CrossRef]
8. Hamaguchi, R.; Yahashi, H.; Nishimura, Y.; Minemoto, M.; Matsukuma, Y.; Watabe, M.; Arikawa, K. Fluid dynamic study on recovery system of methane hydrate. In *Asian Pacific Confederation of Chemical Engineering Congress Program and Abstracts*; The Society of Chemical Engineers: Osaka, Japan, 2004; pp. 1–8.
9. Mech, D.; Gupta, P.; Sangwai, J.S. Kinetics of methane hydrate formation in an aqueous solution of thermodynamic promoters (THF and TBAB) with and without kinetic promoter (SDS). *J. Nat. Gas Sci. Eng.* **2016**, *35*, 1519–1534. [CrossRef]
10. Kawasaki, Y.; Nakano, H. Development of simplified teaching material educating engineering and resource science students in the production of gas hydrates. *J. JSEE* **2014**, *62*, 57–60. [CrossRef] [PubMed]
11. Liu, Y.; Ri, I.; Kurihara, M. Researches on stabilization of methane hydrate reservoir by grout material. *J. Jpn. Assoc. Pet. Technol.* **2020**, *85*, 205–225. [CrossRef]
12. Liu, Y.; Ito, K.; Kurihara, M. Experimental designs of arti ficial hydrated cores produced by *iso*-Butane and elucidation of behaviors of gas phase during the stabilization of methane hydrate reservoir by grout material. *J. Jpn. Assoc. Pet. Technol.* **2023**, *88*, 105–122. [CrossRef]
13. Shibata, I. Flow characteristics of cement grout for dam-foundation rock in small tubes. *Proc. Jpn. Soc. Civ. Eng.* **1992**, *453*, 107–116. (In Japanese)
14. Yamamoto, K.; Yoneda, J.; MH21 Working Group. Mechanical response of the formation—Formation stability and sand problem mechanism. In Proceedings of the Methane Hydrate Forum 2014, Tokyo, Japan, 25 November 2014. (In Japanese).
15. Suzuki, K.; Narita, H. Estimation of Permeability of methane hydrate-bearing strata of Nankai Trough, in comparison to core measurement vs. CMR analysis. *J. Jpn. Assoc. Pet. Technol.* **2010**, *75*, 98–105. [CrossRef]
16. Gas Encyclopedia Website by Air Liquide: 030-Isobutane. Available online: https://encyclopedia.airliquide.com/isobutane (accessed on 11 September 2020).
17. Buleiko, V.M.; Grigoriev, B.A.; Mendoza, J. Calorimetric investigation of hydrates of pure isobutane and *iso*- and normal butane mixtures. *Fluid Phase Equilibria* **2018**, *462*, 14–24. [CrossRef]
18. Hayano, I.; Uchida, T. Generation observation and thermodynamic properties of iso-butane. *Kogyō Kagaku Zassi J. Chem. Soc. Jpn. Ind. Chem. Sect.* **1964**, *67*, 997–999. (In Japanese)
19. Guo, X.; Jin, Y.; Zi, J.; Lin, J.; Zhu, B. A 3D modeling study of effects of heterogeneity on system responses in methane hydrate reservoirs with horizontal well depressurization. *Gas Sci. Eng.* **2023**, *115*, 205001. [CrossRef]
20. Yamamoto, K.; Fujii, T.; Nagao, J.; Nakatsuka, Y. Methane hydrate: The 1st subsea production test. In Proceedings of the Methane Hydrate Forum 2013, Tokyo, Japan, 24 January 2014. (In Japanese)